MOLECULAR AND CELLULAR BIOLOGY, Mar. 1996, p. 1017–1026 Vol. 16, No. 3
0270-7306/96/$04.00+0

A Novel Histone H4 Mutant Defective in Nuclear Division and Mitotic Chromosome Transmission

M. MITCHELL SMITH,* PEIRONG YANG, MARIA SOLEDAD SANTISTEBAN, PAUL W. BOONE, ANDREW T. GOLDSTEIN, AND PAUL C. MEGEE†

Department of Microbiology and University of Virginia Cancer Center, School of Medicine, University of Virginia, Charlottesville, Virginia 22908

Received 14 July 1995/Returned for modification 5 September 1995/Accepted 30 November 1995

The histone proteins are essential for the assembly and function of the eukaryotic chromosome. Here we report the first isolation of a temperature-sensitive lethal histone H4 mutant defective in mitotic chromosome transmission in *Saccharomyces cerevisiae*. The mutant requires two amino acid substitutions in histone H4: a lethal Thr-to-Ile change at position 82, which lies within one of the DNA-binding surfaces of the protein, and a substitution of Ala to Val at position 89 that is an intragenic suppressor. Genetic and biochemical evidence shows that the mutant histone H4 is temperature sensitive for function but not for synthesis, deposition, or stability. The chromatin structure of 2μm circle minichromosomes is temperature sensitive in vivo, consistent with a defect in H4-DNA interactions. The mutant also has defects in transcription, displaying weak Spt$^-$ and Sin$^-$ phenotypes. At the restrictive temperature, mutant cells arrest in the cell cycle at nuclear division, with a large bud, a single nucleus with 2C DNA content, and a short bipolar spindle. At semipermissive temperatures, the frequency of chromosome loss is elevated 60-fold in the mutant while DNA recombination frequencies are unaffected. High-copy *CSE4*, encoding an H3 variant related to the mammalian CENP-A kinetochore antigen, was found to suppress the temperature sensitivity of the mutant without suppressing the Spt$^-$ transcription defect. These genetic, biochemical, and phenotypic results indicate that this novel histone H4 mutant defines one or more chromatin-dependent steps in chromosome segregation.

Determining the functional properties of the eukaryotic nucleosome in vivo remains an important and challenging problem in molecular genetics. The nucleosome is a complex macromolecular structure composed of a core octamer of histone protein and 146 bp of DNA wound in approximately 1.8 left-handed superhelical turns around the surface of the histones (42, 79, 83, 89). The structure of the core histone octamer has been determined from high-resolution X-ray crystal data (2), and a molecular model of the structure of the nucleosome has been proposed by Arents and Moudrianakis (3).

In metazoan cells, the genetic analysis of histone function is complicated by the fact that there are generally many copies of the genes for each major histone. However, in *Saccharomyces cerevisiae*, there are only two copies of each of the core histone genes per haploid genome, and these nonallelic gene copies can be individually deleted or disrupted, making possible the construction and genetic analysis of mutant alleles (41, 57, 71, 77, 80).

The construction of yeast histone gene mutations in vitro has proven to be a powerful approach to genetic analysis of a variety of functions, particularly RNA transcription. Experiments with deletions and site-directed point mutations have identified specific sequences within the N-terminal domains of histones H3 and H4 required for both transcriptional gene activation and gene repression (1, 18, 26, 37–39, 48, 51, 60, 70). Random mutagenesis and forward genetic screens have identified additional new core histone mutants that suppress the loss of global transcriptional activators (27, 42a, 65) or block their function (29), suggesting a dependent pathway of activation steps involving chromatin structure (29; reviewed in reference 88).

Analyses of other histone mutants have shown that they play functional roles in sporulation and nuclear division (51, 54, 60). Recently, mutational studies have uncovered a new role for histone H4 in the maintenance of genome integrity. Creation of point mutations in the lysines subject to reversible acetylation identified a novel lysine-dependent function that, when disrupted, results in increased DNA damage, activation of the *RAD9*-dependent cell cycle checkpoint, and induction of DNA damage-inducible gene expression (52).

In the work reported here, we have focused on the role of the histones in mitotic chromosome transmission. A growing body of evidence supports the hypothesis that the histones perform critical functions in mitosis, where replicated sister chromatids must undergo a complex set of structural changes, attach to the spindle apparatus, and disjoin to mother and daughter cells. Gross depletion of either H2B (22) or H4 (40, 54) results in cell death, starting in S phase, with cells finally arresting at the G_2 to M transition, suggesting essential roles for these histones in DNA replication, mitosis, or both. More specifically, alterations in histone gene dosage have been shown to increase frequencies of mitotic chromosome loss in both native chromosomes and circular minichromosomes (50, 80).

Biochemical and genetic studies of centromere and telomere chromatin also suggest that the histones might play important roles in segregation. Early work by Bloom and Carbon (8) showed that yeast centromeres are packaged into a unique chromatin structure composed of a nuclease-resistant core flanked by ordered arrays of nucleosomes (7, 20). Furthermore, there is a strong correlation between the integrity of this chromatin structure and centromere function (74, 75). The

* Corresponding author. Mailing address: Department of Microbiology and University of Virginia Cancer Center, Box 441, Jordan Bldg., School of Medicine, University of Virginia, Charlottesville, VA 22908. Phone: (804) 924-2669. Fax: (804) 982-1071. Electronic mail address: mms7r@Virginia.EDU.

† Present address: Department of Embryology, The Carnegie Institute of Washington, Baltimore, MD 21210.

TABLE 1. Yeast strains used

Strain	Relevant genotype	Source or reference
MSY168	*MAT***a**/*MAT*α *ura3-52*/*ura3-52 ade2-101*/*ade2-101 HHT1-HHF1*/Δ(*hht1-hhf1*) Δ(*hht2-hhf2*)/*HHT2-HHF2*	80
MX4-22A	*MAT***a** *ura3-52 leu2-3,112 lys2-Δ201* Δ(*hht1-hhf1*) Δ(*hht2-hhf2*) pMS329[*CEN4 ARS1 URA3 HHT1 HHF1*]	51
MSY-P1I8	*MAT***a** *ura3-52 leu2-3,112 lys2-Δ201* Δ(*hht1-hhf1*) Δ(*hht2-hhf2*) pMS337[*CEN4 ARS1 LEU2 HHT1 HHF1*]	51
MSY-P3B4	*MAT***a** *ura3-52 leu2-3,112 lys2-Δ201* Δ(*hht1-hhf1*) Δ(*hht2-hhf2*) pMS340[*CEN4 ARS1 LEU2 HHT1 hhf1-12*]	This work
MSY-P3B6	*MAT***a** *ura3-52 leu2-3,112 lys2-Δ201* Δ(*hht1-hhf1*) Δ(*hht2-hhf2*) pMS343[2μm *LEU2 HHT1 hhf1-12*]	This work
MSY-P726	*MAT***a** *ura3-52 leu2-3,112 lys2-Δ201* Δ(*hht1-hhf1*) Δ(*hht2-hhf2*) pMS352[*CEN4 ARS1 LEU2 HHT1 hhf1-20*]	This work
MSY861	*MAT***a** *his4-912*δ *lys2-128*δ *ura3-52 leu2-3,112* Δ(*hht1-hhf1*) Δ(*hht2-hhf2*) pMS337[*CEN4 ARS1 LEU2 HHT1 HHF1*]	This work
MSY862	*MAT***a** *his4-912*δ *lys2-128*δ *ura3-52 leu2-3,112* Δ(*hht1-hhf1*) Δ(*hht2-hhf2*) pMS352[*CEN4 ARS1 LEU2 HHT1 hhf1-20*]	This work
MSY827	*MAT***a** *his4-912*δ *lys2-128*δ *ura3-52 leu2-3,112* Δ(*hht1-hhf1*) Δ(*hht2-hhf2*) pMS352[*CEN4 ARS1 LEU2 HHT1 hhf1-20*] pPY3-4[2μm *URA3 CSE4*]	This work
MSY768	*MAT***a** *his4-912*δ *lys2-128*δ *ura3-52 LEU2*::(*HHT1 hhf1-37*) Δ(*hht1-hhf1*) Δ(*hht2-hhf2*)	This work
MSY743	*MAT***a** *ura3-52 lys2-Δ201 snf2*::*URA3 LEU2*::(*HHT1 HHF1*) Δ(*hht1-hhf1*) Δ(*hht2-hhf2*)	This work
MSY863	*MAT***a** *ura3-52 leu2-3,112 lys2-Δ201 snf2*::*URA3* Δ(*hht1-hhf1*) Δ(*hht2-hhf2*) pMS352[*CEN4 ARS1 LEU2 HHT1 hhf1-20*]	This work
MSY749	*MAT***a** *ura3-52 lys2-Δ201 snf2*::*URA3 LEU2*::(*HHT1 hhf1-37*) Δ(*hht1-hhf1*) Δ(*hht2-hhf2*)	This work
L3703	*MAT***a** *ura3-52 gcn4-2 bas1-2 bas2-2 sit1-4*	4
MX15-3B	*MAT***a** *ura3-52 leu2-3,112 gcn4-2 bas1-2 bas2-2* Δ(*hht1-hhf1*) Δ(*hht2-hhf2*) pMS329[*CEN4 ARS1 URA3 HHT1 HHF1*]	This work
MSY864	*MAT***a** *ura3-52 leu2-3,112 gcn4-2 bas1-2 bas2-2* Δ(*hht1-hhf1*) Δ(*hht2-hhf2*) pMS352[*CEN4 ARS1 LEU2 HHT1 hhf1-20*]	This work

centromeres of the fission yeast *Schizosaccharomyces pombe* are also assembled in a specialized chromatin structure, which probably plays an important role in their function (49, 64). Telomeres are also organized into distinct nucleosomal and nonnucleosomal chromatin structures (90), and chromatin-associated proteins, including histones, are essential for telomere function (1, 26, 53). Some of these may be important for the role of telomeres in mitotic chromosome transmission (47, 73). Potentially, the histones could participate in many other steps necessary for mitotic chromosome transmission in addition to centromere and telomere function, such as the resolution of replicated chromatids by topoisomerases (31, 32), the maintenance of sister chromatid cohesion, or the condensation of mitotic chromosomes (21).

To obtain a better understanding of the functions of the histones in chromosome segregation, we undertook a forward genetic screen to identify conditional lethal histone mutants specifically defective in nuclear division. In this report, we describe the isolation of a novel cell division cycle histone H4 mutant that arrests at nuclear division. Under semipermissive conditions, the mutant has a 50- to 60-fold increase in the frequency of chromosome loss but a normal level of recombination. Together, these results define a specific role for histone H4 in mitotic chromosome transmission, and we propose that this role involves centromere chromatin structure and function.

MATERIALS AND METHODS

Strains and plasmids. The relevant genotypes of yeast strains used in this study are listed in Table 1. Plasmid pMS302, described previously (51), is a *CEN4*/*ARS1*/*URA3*/*SUP11* yeast vector containing the wild-type copy-I histone H3 gene (*HHT1*) and a *Bam*HI synthetic oligonucleotide linker in place of a deletion of the copy-I histone H4 gene (*HHF1*). The linker provides a unique *Bam*HI site in which to clone test alleles of *HHF1*. Plasmids pMS329 and pMS368 are derivatives of plasmid pMS302 containing *HHF1* and *hhf1-12*, respectively. Plasmid pMS343 is a high-copy-number 2μm LEU2 vector containing the *HHT1* and *hhf1-12* gene pair from mutant *ts*19. It was constructed by subcloning the *Eco*RI-*Hin*dIII fragment from pMS368 into plasmid pVB100 (kindly provided by Vivian Berlin). Plasmid pMS347, described previously (51), is a *CEN4*/*ARS1*/*LEU2* vector that contains wild-type *HHT1* and a deletion of *HHF1*, the same derivative of the copy-I histone locus as pMS302. Plasmids pMS337, pMS340, and pMS352 are derivatives of plasmid pMS347 that contain *HHF1*, *hhf1-12*, and *hhf1-20*, respectively.

Mutagenesis and library construction. The substrate for mutagenesis of *HHF1* was a 476-bp *Rsa*I subclone in bacteriophage M13mp7, described previously (51). A single-stranded DNA template of *HHF1* was mutagenized in vitro with sodium bisulfite as described previously (76, 78, 84). This mutagenized template was converted to double-stranded DNA by primer-directed polymerization with the Klenow fragment of DNA polymerase I. The double-stranded H4 gene fragment was isolated as a 488-bp *Bam*HI fragment and subcloned into plasmid pMS302 at its unique *Bam*HI site. In the correct orientation, the cloned H4 fragment recreates an H3-H4 gene pair capable of proper expression in *S. cerevisiae* (51, 54). Plasmid DNA libraries were prepared from pools of approximately 1,000 bacterial colonies. Oligonucleotide mutagenesis was carried out as described previously with an M13mp8 subclone of the 488-bp histone H4 *Bam*HI fragment (43, 51).

Mutant screens. A meiotic segregation protocol was used to screen for mutants by plasmid rescue as described previously (78). The diploid yeast host MSY168 was transformed with the pMS302 plasmid library of mutagenized *HHF1* fragments selecting for Ura^+ colonies. Pooled yeast transformants were then sporulated to produce haploid segregants in which a member of the pMS302 plasmid library provided the only source of histones H3 and H4. These were identified as nonsectoring white colonies that were unable to grow on medium containing 5-fluoroorotic acid (10, 28, 78). Haploid isolates rescued by the library plasmid were then picked and screened for those that were unable to grow at the restrictive temperature of 37°C.

Plasmid shuffle experiments were carried out as described previously (10, 51, 78). Yeast strain MX4-22A containing plasmid pMS329 was transformed with a second plasmid derived from pMS347 containing the target H4 gene. Mitotic segregants that lost the original pMS329 plasmid were then selected on 5-fluoroorotic acid medium (9). The result of this shuffle protocol was the replacement of plasmid pMS329 with a new plasmid containing the test allele of histone H4.

Cell growth and division analysis. The growth of cells in liquid culture was monitored by cell counts with a Coulter model ZM particle counter. Cell volume histograms were collected with a Coulter model C256 pulse height analyzer. Nuclear morphology was determined by staining with 4′,6-diamidino-2-phenylindole (DAPI) as described previously (86). Flow cytometry was carried out on cells fixed with ethanol and stained with propidium iodide as described previously (17, 78). For G_1 arrest, cells were blocked by nitrogen starvation, as described previously (13), until more than 85% of cells were unbudded.

Micrococcal nuclease digestion. Yeast nuclei were prepared as described previously (13, 46) and resuspended in 1.1 M sorbitol–0.02 M piperazine-*N*,*N*′-bis(2-ethanesulfonic acid) (PIPES; pH 6.3)–0.5 mM $CaCl_2$. Samples were prewarmed to 37°C for 2 min, and micrococcal nuclease was added to give 1, 3, 10, and 30 U/ml. After a 5-min incubation, the reactions were stopped by adjusting to 20 mM EDTA and 1% sodium dodecyl sulfate (SDS). DNA fragments were purified by phenol-chloroform extraction and resolved by electrophoresis on 1% agarose.

Analysis of DNA topoisomers. The topoisomer distribution of the yeast 2μm circle plasmid DNA was assayed as described previously (72). Cells were rapidly shifted from 28 to 37°C by the addition of an equal volume of medium prewarmed to 46°C. Samples were removed at intervals after the shift, and cells were collected rapidly by filtration. DNA was prepared by breaking the cells with glass beads in the presence of phenol while maintaining the temperature at 37°C (72). Topoisomers were separated by electrophoresis in 1.2% agarose gels containing 1.75 μg of chloroquine per ml (69) and detected by blot hybridization with radiolabeled 2μm circle DNA as a probe. The Southern blots were quantified with a Molecular Dynamics PhosphorImager, and the mean topoisomer distribution of each sample was determined by least-squares nonlinear curve fitting to a Gaussian distribution.

Purification of histones. Yeast nuclei were prepared as described previously (13, 46). Crude nuclei were washed three times in ice-cold buffer A (10 mM

Tris-HCl [pH 8.0], 0.5% Nonidet P-40, 75 mM NaCl, 1 mM phenylmethylsulfonyl fluoride) and resuspended in buffer B (10 mM Tris-HCl [pH 8.0], 0.4 M NaCl, 1 mM phenylmethylsulfonyl fluoride). One-tenth volume of 4 M H_2SO_4 was added slowly with stirring, and histones were extracted for 30 min on ice. Insoluble material was pelleted by centrifugation at 25,000 × *g* for 15 min and re-extracted three times in buffer B plus 0.4 M H_2SO_4. Histones were precipitated with 5 volumes of acetone, washed with acetone, and dried.

RESULTS

Cell division cycle (*cdc*) mutants blocked at nuclear division have a uniform and recognizable morphology in *S. cerevisiae*: single cells with a large daughter bud and a single undivided nucleus (68). Taking advantage of this simple morphological screen, we sought to isolate histone H4 mutants specifically defective in steps required for mitotic chromosome segregation. Our strategy was to randomly mutate the cloned histone H4 gene *HHF1* in vitro and then introduce this DNA into yeast cells such that it provided the only source of histone H4 expression. This yeast library was screened for temperature-sensitive colonies, and then these isolates were examined individually for those that gave a uniform *cdc* terminal phenotype characteristic of arrest at nuclear division.

Isolation of *ts*19. The coding sequence of *HHF1* was randomly mutated in vitro by using sodium bisulfite to generate C-to-T transitions in the noncoding strand of the gene. A yeast library expressing the mutagenized histone H4 genes was constructed in two steps. First, MSY168, a diploid strain hemizygous for both of the nonallelic chromosomal histone H3-H4 loci, was transformed with the treated plasmid DNA. Then this population was sporulated to produce segregants in which the plasmid-borne *hhf1* gene served as the sole source of histone H4 (see Materials and Methods). Thirteen temperature-sensitive mutants were identified in a screen of approximately 12,000 colonies. At the restrictive temperature, two of these mutants accumulated as large budded cells with a single nucleus, suggesting a specific cell division cycle defect at nuclear division. Subsequent DNA sequence analysis showed that the histone H4 genes in these two strains had identical nucleotide substitutions, indicating that they arose as sibling plasmids during propagation in bacteria or yeasts. One of the isolates, named *ts*19, was selected for further study.

Subcloning and linkage analysis of the plasmid recovered from *ts*19 confirmed that the temperature-sensitive phenotype of *ts*19 was caused by the mutant allele of histone H4, designated *hhf1-12*, and not a mutation in an unrelated gene elsewhere in the *ts*19 genome or in the plasmid. The temperature-sensitive phenotype of *hhf1-12* constructs is shown in Fig. 1. Cells with either low-copy or high-copy plasmid derivatives of *hhf1-12* are temperature sensitive for growth, showing that the histone H4 defect cannot be corrected by an increased gene dosage of the mutant allele. The *hhf1-12* H4 mutation is recessive in that cells are able to grow at the restrictive temperature when they carry two plasmids, one with *hhf1-12* and the other with wild-type *HHF1* (data not shown).

DNA sequence analysis of *hhf1-12* identified 11 C-to-T transitions, 4 of which resulted in amino acid substitutions: Ser to Phe at position 1 (S1F), His to Tyr at position 18 (H18Y), Thr to Ile at position 82 (T82I), and Ala to Val at position 89 (A89V). To determine which of the four amino acid substitutions was responsible for the temperature-sensitive phenotype of *ts*19, the individual mutations were reconstructed one at a time by site-directed oligonucleotide mutagenesis and scored by a plasmid shuffle protocol (10). The expected conditional-lethal phenotype was not recovered with any of the four single amino acid substitutions. Three of the mutations, S1F, H18Y, and A89V, produced cells that were wild type for growth at 37°C. However, cells with the T82I mutation were not recovered at all, showing that this allele is either lethal or extremely detrimental (78). Previous experiments with point mutations in the N-terminal domain of histone H4 (51) suggested that the substitutions at positions 1 and 18 were unlikely to be responsible for the phenotype of *ts*19. Therefore, we next constructed the T82I-A89V double substitution allele, called *hhf1-20*. Mutants expressing this allele were viable and grew as well as the original *ts*19 strain at permissive temperatures but failed to form colonies at the restrictive temperature of 37°C (Fig. 1). Thus, the phenotype of *ts*19 depends on two amino acid substitutions in *HHF1*: the T82I change, which is lethal, and the A89V change, which acts as an intragenic suppressor at permissive temperature.

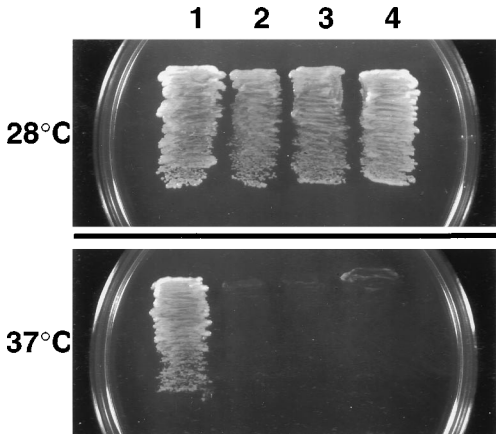

FIG. 1. Conditional growth of histone H4 mutants. The growth phenotypes of the wild-type parent and histone H4 mutants at permissive (28°C) and restrictive (37°C) temperatures are shown. Cells were streaked on agar plates and grown for 2 days at the indicated temperatures. All four strains were isogenic except for the particular histone H4 expression plasmid they each contained. Lanes: 1, pMS337 (*HHF1*); 2, pMS340 (*hhf1-12*); 3, pMS343 (high-copy *hhf1-12*); 4, pMS352 (*hhf1-20*).

Structure of substitutions. The lethal T82I substitution resides within the short beta-sheet region between helices 2 and 3 of the H4 histone fold (2). There is strong biochemical evidence from cross-linking and chemical protection experiments that this short beta-sheet region forms a DNA-binding surface in the nucleosome (6, 44). In addition, recent molecular modeling studies indicate that this short beta-sheet region in histone H4 is one of the "paired-element motifs" that form the DNA-binding surfaces of the histone octamer (2, 3). A feature of these paired-element motifs is the presence of hydroxyl-containing amino acids, usually serine or threonine, capable of making contact with phosphates on the inward-facing surface of the DNA helix (2, 3). The A89V substitution is within the helix 3 domain of the H4 histone fold, and this mutation alone does not present a detectable phenotype. We hypothesize that the T82I substitution lethally disrupts the DNA-binding surface across the paired element motif of the two histone H4 molecules in the octamer. The A89V mutation then serves as an intragenic suppressor to alter the structure of histone H4 sufficiently to provide an acceptable path for the DNA at permissive but not restrictive temperatures.

Temperature-sensitive phenotype. Before undertaking a biochemical analysis of histone H4 and chromatin in *hhf1-20*, we sought an estimate of the phenotypic lag of mutant cells, that is, the length of time it takes to establish the mutant phenotype following a shift to the restrictive temperature. The significance of biochemical results, particularly negative results, prior

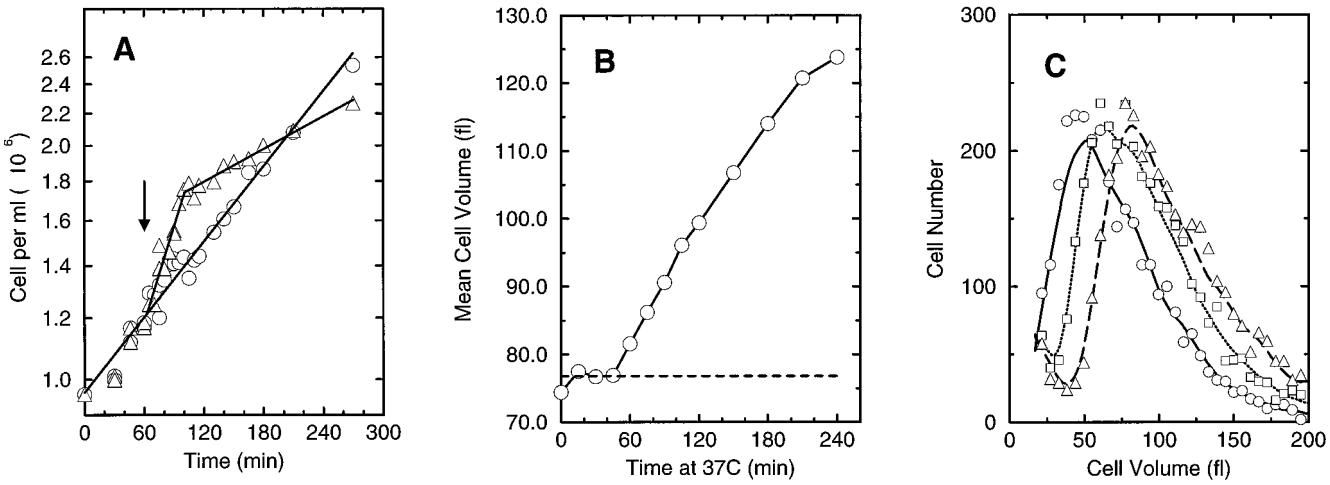

FIG. 2. Temperature-sensitive phenotype of *hhf1-20*. (A) Kinetics of cell division. A culture of *hhf1-20* growing exponentially at 28°C (○) was split, and half was shifted to 37°C (□) at 60 min, indicated by the arrow. At the time of the shift, there was a brief increase in cell number; this was followed 40 to 60 min later by a sharply reduced rate of division. (B) Mean cell volume. A culture of *hhf1-20* cells growing exponentially at 28°C was shifted to 37°C at 0 min. The mean cell volume of the culture was monitored over time after the shift (○). The dashed line indicates the mean cell volume of the control culture retained at 28°C. After a lag of 40 to 60 min, there was a steady increase in mean cell volume with time, reflecting an imbalance between growth and cell division. (C) Cell volume histograms for the experiment presented in panel B. Symbols: ○, 0 min; □, 90 min; △, 150 min.

to this time is unclear. Once the mutant phenotype is established, however, the primary molecular defects that produce the temperature sensitivity of *hhf1-20* must have occurred.

The effect of shifting an exponentially growing culture of *hhf1-20* cells to the restrictive temperature is shown in Fig. 2A. At the permissive temperature, the generation time of *hhf1-20* cells is approximately 175 min. At the time of the shift, there is a short period of more rapid increase in the cell number. Then, about 40 to 60 min later, the population changes to a much longer doubling time of about 490 min. Maintained at the restrictive temperature, the cells continue to divide at this retarded rate, eventually dying after a few additional prolonged cell divisions. Thus, the mutant growth phenotype is evident in the culture within 40 to 60 min of increasing the temperature. This estimate of phenotypic lag is supported by the change in cell volume of the mutant following a shift to the restrictive temperature (Fig. 2B). This change in volume reflects the imbalance between cell growth and division in the H4 mutant; individual cells continue to grow at the restrictive temperature but have a retarded rate of cell division and therefore continually increase in size. As can be seen in Fig. 2B, approximately 40 to 60 min following the shift to the restrictive temperature, the mutant phenotype is evident as a steady rate of increase in the mean cell volume of the population. From the histograms of cell volume versus time (Fig. 2C), it is clear that this mutant growth phenotype is displayed by the entire cell population. As described below, a uniform delay phenotype in the first cell division cycle was confirmed by using synchronous cultures.

On the basis of the kinetics of the change in minichromosome linking number, described below, it is likely that the phenotypic lag of *hhf1-20* is considerably less than 40 to 60 min. An alternate interpretation of the delay is that it reflects a specific temperature-sensitive step in the cell division cycle (23, 66, 67); at the time of the shift, cells that are past the transition point continue to complete a normal mitosis for approximately 40 to 60 min while those that have not reached the transition point are severely delayed. Experiments to test this prediction are in progress. In any case, 60 min is a maximum estimate of the phenotypic lag of *hhf1-20*, after which time the biochemistry of the cellular chromatin should reflect the mutant state.

Chromatin structure and DNA linking number. The positions of the amino acid substitutions in *hhf1-20* predicted that its chromatin structure should be temperature sensitive. To test this prediction, we first examined the overall chromatin structure of *hhf1-20* by micrococcal nuclease digestion of nuclei prepared from cells grown at restrictive temperature for 3 h. As seen in Fig. 3, a typical nucleosome DNA repeat ladder is seen with either *HHF1* or *hhf1-20* at both permissive and restrictive temperatures. These results are distinct from those obtained with conditional null mutants of H2B or H4, in which histone depletion results in a severe loss of oligonucleosome DNA fragments (22, 40), and they suggest that the phenotype of *hhf1-20* is not due to a general depletion of histone H4.

We next examined the DNA linking number of the naturally occurring yeast 2μm circle plasmid, which exists as a covalently closed circular minichromosome assembled into nucleosomal chromatin (for a review, see reference 12). The DNA linking number of 2μm circle DNA, as with other closed circular

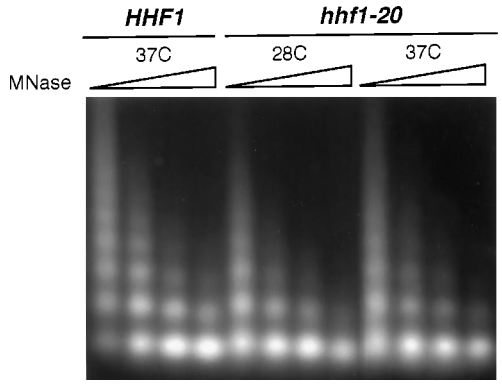

FIG. 3. Micrococcal nuclease assays of *hhf1-20* chromatin. Cells were grown at either 28°C (*hhf1-20*) or 37°C (*HHF1* and *hhf1-20*) for 3 h, and nuclei were prepared. Nuclei were then digested with increasing concentrations of nuclease (MNase) indicated by the concentration ramp shown at the top of each set of lanes (1, 3, 10, and 30 U/ml). The resulting nucleosome DNA fragments were purified, separated by gel electrophoresis, and visualized by ethidium bromide staining.

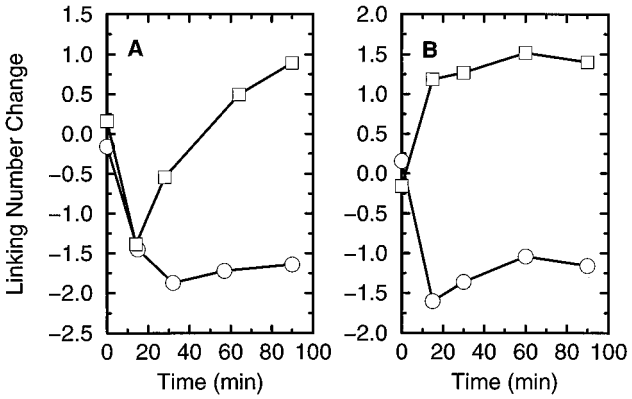

FIG. 4. Superhelical density of 2μm circle chromatin DNA. (A) Exponentially growing cultures. The change in mean linking number of 2μm circle DNA is shown as a function of the time after a shift from 28 to 37°C. (B) Cultures arrested in G_1. The data for cells arrested by nitrogen starvation are shown as in panel A. Symbols: ○, *HHF1*; □, *hhf1-20*.

chromosomes, is sensitive to changes in chromatin structure (11, 22, 35, 36, 40, 45, 59, 61, 72). For these experiments, cultures of *HHF1* and *hhf1-20* were shifted to the restrictive temperature and DNA was prepared at intervals after the shift. Since the cells in the two cultures were isogenic with the exception of the histone H4 alleles, any differences in the response of 2μm circle chromatin to temperature must be due, directly or indirectly, to the mutant histone H4 protein. Topoisomers of 2μm circle plasmid were separated by electrophoresis in chloroquine-agarose gels (69) and visualized by Southern hybridization. The mean of each distribution was estimated by fitting the integrated intensity of the topoisomer bands to a Gaussian curve, and the kinetics of the change in linking number was examined after shifting cells to the restrictive temperature. The results for exponentially growing cultures are shown in Fig. 4A. When wild-type *HHF1* cells are shifted from 28 to 37°C, there is a rapid change in the topoisomer distribution of 2μm circle DNA toward decreased linking number. This change is expected because of the thermal unwinding of the DNA unconstrained by nucleosomes and is in excellent agreement with previous results (56, 72). In contrast, when cells expressing *hhf1-20* are shifted to the restrictive temperature, there is an initial decrease in linking number, but then it increases with time until by 90 min the mean topoisomer distributions of 2μm circle DNAs from *HHF1* and *hhf1-20* differ by about 2.5 superhelical turns.

These results suggested that *hhf1-20* cells have an unusual temperature-sensitive chromatin structure. However, since *hhf1-20* cells arrest at G_2-M at the restrictive temperature whereas *HHF1* cells continue to cycle, it was possible that the difference in chromatin structure reflected the arrest of *hhf1-20* cells at a time in the division cycle when the 2μm circle chromatin might be naturally in a more relaxed state (55). Therefore, we next examined the structure of the 2μm circle in cells blocked in G_1 by nitrogen starvation (13, 68). The results of this experiment are shown in Fig. 4B. Wild-type *HHF1* cells again exhibited the expected decrease in linking number as a result of thermal unwinding when shifted to 37°C. Despite being arrested in G_1, the topoisomer distribution of *hhf1-20* again increased in linking number at the restrictive temperature. In this experiment, the change in distribution occurred within 15 min of the shift in temperature. The magnitude of the difference between *HHF1* and *hhf1-20* was about 2.6 superhelical turns, virtually identical to that of cycling cells. Thus, the change in 2μm circle chromatin structure is a property of the mutant histone H4 and not of the arrest point of the mutant cells. Furthermore, since the alteration in chromatin structure takes place in the absence of any cell cycle progression and in G_1 prior to any DNA replication or histone synthesis, the mutant phenotype must result from a defect in either histone H4 function or stability and not in synthesis or deposition.

TABLE 2. Viability of *hhf1-20* at the restrictive temperature

Time at 37°C (min)	Plating efficiency (%)
0	100
120	98
170	93
300	71
405	73
1,080	15

Stability of the mutant protein. Several observations suggested that the mutant H4 protein was stable. As noted above, expression of *hhf1-12* from a high-copy-number plasmid did not suppress the temperature-sensitive phenotype of the mutant (Fig. 1) as might be expected if the protein were simply unstable (16, 50). In addition, *hhf1-20* cells arrested at nuclear division at the restrictive temperature retained high viability for extended periods (Table 2). This result is distinct from that seen with histone depletion, when cells begin an irreversible death starting in S phase (22, 40). The stability of the *hhf1-20* H4 protein was confirmed by biochemical analysis of the histones. An *HHF1* wild-type strain and an *hhf1-20* mutant strain, isogenic except for their histone H4 genes, were shifted to 37°C for 2 h, and histone proteins were prepared from each. As shown in Fig. 5, the histone compositions of the two chromatins were identical; both contained histone H4 protein and in the same amounts relative to the other histones. Thus, the mutant H4 protein is not degraded at the restrictive temperature and therefore the mutant phenotype must be the result of a defect in H4 function.

Transcription phenotypes of *hhf1-20*. We examined *hhf1-20* for gene transcription phenotypes by three well-characterized assays: (i) suppression of Ty1 solo δ insertion mutations (19, 88); (ii) suppression of mutations in the SNF-SWI complex (27, 30, 65); and (iii) suppression of deletions in promoter-specific transcription activation factors (4). These assays were carried out at both permissive and semipermissive temperatures. We found that all the detected phenotypes were insensitive to growth temperature.

Yeast strains that carry *his4-912*δ and *lys2-128*δ alleles are auxotrophic for histidine and lysine, respectively, because the genes are inactivated by solo δ elements remaining from Ty1

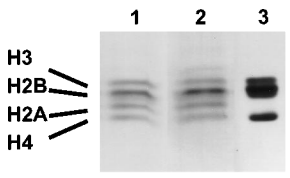

FIG. 5. Histone composition of wild-type and mutant nuclei. Yeast strains isogenic except for their histone H4 expression plasmids were grown at 28°C until mid-logarithmic growth and then shifted to the restrictive temperature of 37°C for 2 h. Histones were extracted from both cultures and separated by SDS-polyacrylamide gel electrophoresis together with marker histones from calf thymus. Lanes: 1, *HHF1* wild type; 2, *hhf1-20* mutant; 3, calf thymus histones.

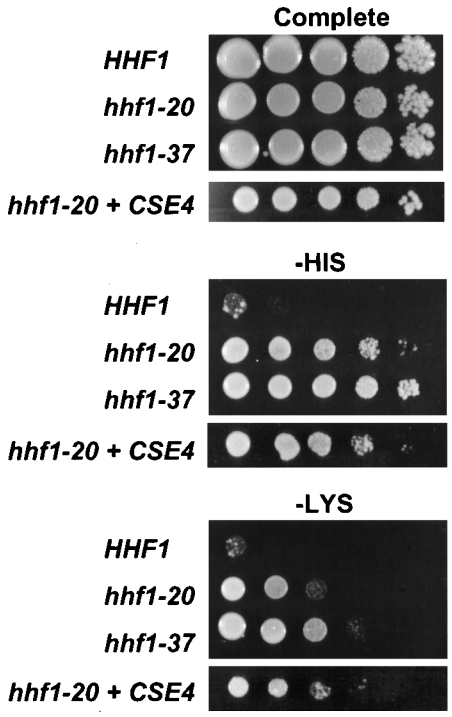

FIG. 6. Suppression of Ty1 solo δ insertions. Tenfold serial dilutions of *his4-912*δ *lys2-128*δ strains with the indicated histone H4 genotypes were spotted onto plates containing either complete medium (Complete), synthetic complete medium minus histidine (−HIS), or synthetic complete medium minus lysine (−LYS). Both *hhf1-20* and *hhf1-37* are able to suppress *his4-912*δ and weakly suppress *lys2-128*δ. High-copy *CSE4* does not alter the *spt*-like phenotype of *hhf1-20*. The strains used were MSY861 (*HHF1*), MSY862 (*hhf1-20*), MSY768 (*hhf1-37*), and MSY827 (*hhf1-20* + *CSE4*).

transposon insertions (19, 88). The histone genes are among the "suppressors of Ty1" (*SPT* genes) that restore the function of *his4-912*δ and *lys2-128*δ by altering promoter selection. High gene dosages of wild-type H2A-H2B or H3-H4 gene pairs or decreased gene dosages of H2A-H2B are all able to suppress the solo δ insertions and cause reversion of the Lys^- and His^- phenotypes (16). To test *hhf1-20* for Spt^- phenotypes, we introduced either wild-type *HHF1*, *hhf1-20*, or *hhf1-37* into a *his4-912*δ *lys2-128*δ strain by plasmid shuffle. The *hhf1-37* allele causes a Tyr-to-Gly substitution at position 88 and served as a positive control for the Spt^- phenotype (73a). As can be seen in Fig. 6, all the strains grew well on complete medium but *HHF1* failed to grow in the absence of histidine (−HIS) or lysine (−LYS), as expected, because of the solo δ insertions in *his4-912*δ and *lys2-128*δ. Both *hhf1-37* and *hhf1-20* were able to suppress *his4-912*δ relatively well and confer growth in the absence of histidine, although *hhf1-20* was the weaker of the two suppressor alleles (Fig. 6, −HIS). Both were also able to partially suppress *lys2-128*δ, with *hhf1-20* again being the weaker allele (Fig. 6, −LYS). Thus, *hhf1-20* causes a weak to moderate Spt^- phenotype. This phenotype appears to be an integral property of *hhf1-20*, since the single A89V substitution allele did not have Spt^- suppressor function (data not shown).

In a second test for transcription phenotypes, we examined *hhf1-20* for its ability to suppress the loss of SNF-SWI function. The SNF-SWI complex is a global transcription activation complex thought to function by remodeling chromatin structure and relieving nucleosome repression at the promoters of a large number of genes (14, 15, 62, 63, 87). Changes in gene dosage of the H2A-H2B gene sets and point mutations in either H3 or H4 are able to partially suppress *snf* and *swi* mutants, making activation SNF-SWI independent (*SIN* genes) (27, 30, 42a, 65). The *SNF2* gene encodes one of the subunits of the SNF-SWI complex, and *snf2* mutants are defective for activation of *SUC2* and *INO1*, resulting in an inability to utilize raffinose as a carbon source in the case of *SUC2* or to grow in the absence of inositol in the case of *INO1*. Figure 7 illustrates the growth of *snf2*::*URA3* disruption strains with different histone H4 alleles. The *hhf1-37* mutant served as a positive control for suppression at *INO1* (73a). Neither *hhf1-37* nor *hhf1-20* was able to suppress the loss of SNF-SWI complex function at *SUC2* as assayed by growth on raffinose (Fig. 7A). In contrast, both were able to suppress the growth defect on inositol (Fig. 7B). Therefore, *hhf1-20* has a weak Sin^- transcription phenotype.

Finally, we examined the ability of *hhf1-20* to restore expression of *HIS4* in the absence of specific transcription activation factors (4). Transcription of *HIS4* depends on the products of the *BAS1*, *GRF10* (*BAS2*/*PHO2*), and *GCN4* genes. A *bas1 grf10 gcn4* triple mutant is phenotypically His^- although the *HIS4* gene is intact and capable of full function. Starting with this triple mutant, His^+ revertants have been found with genes encoding general transcription factors, including the two largest subunits of RNA polymerase II (*SIT1*/*RPO21* and *SIT2*/*RPB2*) (4). Figure 8 illustrates the phenotypes of *bas1 grf10 gcn4* triple-mutant strains. In the presence of the wild-type *HHF1* gene, the cells are unable to grow in the absence of histidine. The *sit1-4* strain serves as a positive control for suppression and restores growth of the triple mutant on minimal medium (Fig. 8, −HIS). However, *hhf1-20* does not suppress

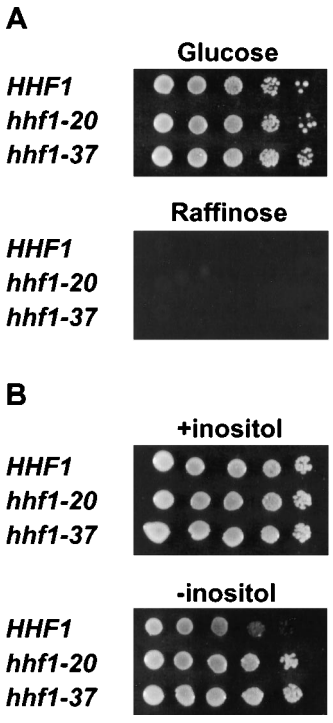

FIG. 7. Suppression of *snf2* mutants. Tenfold serial dilutions of *snf2* disruption strains with the indicated histone H4 genotypes were spotted onto either glucose or raffinose plates (A) or synthetic complete medium with or without inositol (B). Neither *hhf1-20* nor *hhf1-37* was able to suppress the loss of *SNF2* function at *SUC2* (A). Both mutants suppressed the loss of *SNF2* for growth in the absence of inositol (B). The strains used were MSY743 (*HHF1*), MSY863 (*hhf1-20*), and MSY749 (*hhf1-37*).

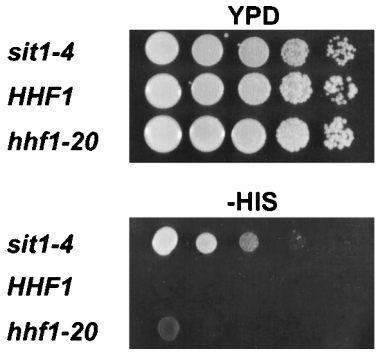

FIG. 8. Suppression of transcription factor mutants. Tenfold serial dilutions of *gcn4-2 bas1-2 bas2-2* triple-mutant strains with the indicated histone H4 genotypes were spotted onto either complete rich medium (YPD) or synthetic complete medium minus histidine (−HIS). The *hhf1-20* mutant did not suppress the loss of expression of *HIS4* in the triple-mutant background. The strains used were L3703 (*sit1-4*), MX15-3B (*HHF1*), and MSY864 (*hhf1-20*).

the lack of expression of *HIS4* in the absence of the normal *trans*-acting factors. Therefore, *hhf1-20* does not cause a Sit^- phenotype.

CDC phenotype of *hhf1-20*. Mutant *ts*19 was originally selected because of its large-bud morphology at the restrictive temperature. A more detailed examination of the CDC phenotype of *hhf1-20* confirmed a severe first-cycle delay at or near the G_2-M boundary. Synchronously dividing cultures of *hhf1-20* were established by selecting small unbudded daughter cells from a balanced growth culture by centrifugal elutriation. One was incubated at the permissive temperature (28°C), and another was incubated at the restrictive temperature (37°C). After 4 h, when the population at the permissive temperature was nearing its second division, the cells at the restrictive temperature had not yet divided (Fig. 9D). Arrested cells were collected after 4 h at the restrictive temperature and examined for cellular morphology. As shown in Fig. 9A to C, *hhf1-20* cells arrested uniformly at the restrictive temperature as large budded cells with a single undivided nucleus and a short bipolar spindle—a terminal phenotype typical of mutants with defects in the replication–nuclear-division pathway (68). DNA histograms for isogenic strains that differed only in their histone H4 alleles are shown in Fig. 10. At the arrest point, *hhf1-20* cells have completed, or nearly completed, DNA replication. Even at the permissive temperature, *hhf1-20* mutants show an increase in the fraction of cells with a 2C DNA content, and this becomes even more pronounced at the restrictive temperature. Taken together, these results show that *hhf1-20* is defective in one or more histone H4-dependent functions necessary to traverse the cell division cycle at a point after DNA replication but before nuclear division.

This terminal phenotype is characteristic of at least two broad classes of defects: those affecting DNA replication and those affecting chromosome segregation (24, 85). To begin to distinguish between these two possibilities, we examined the frequencies of chromosome loss and recombination in *hhf1-20* at the permissive temperature and at the maximal semipermissive temperature compatible with colony formation (24). Mitotic mutants typically have increased frequencies of chromosome loss and roughly wild-type levels of recombination, whereas mutants with mutations in DNA replication show increased frequencies of recombination and smaller increases in chromosome loss (24). The results of assays for chromosome V are shown in Table 3. Cells that were wild type for histone H4 had recombination frequencies of about 2×10^{-4} and loss frequencies of about 3×10^{-5} at the three temperatures tested. These results are consistent with those reported for other wild-type strains (24). At 24 and 28°C, the loss and recombination frequencies of *hhf1-20* were similar to those of the wild type. However, at 35°C, the frequency of chromosome loss in *hhf1-20* increased 50- to 60-fold whereas its recombination frequency was unchanged. Thus, *hhf1-20* most closely resembles the class of G_2 *cdc* mutants including *cdc16* and *cdc20* (24). From these results, it is likely that the lethal defect in *hhf1-20* is in mitosis and not DNA replication.

Suppression of *hhf1-20*. The phenotypic and biochemical analyses of *hhf1-20* suggested two possible mechanisms for the temperature-sensitive mitotic arrest: (i) a direct effect of chromatin structure, and (ii) an indirect effect of aberrant transcription. In the first case, *hhf1-20* might fail to support either proper centromere function or normal alterations in chromosome structure necessary for nuclear division or both. In the second case, *hhf1-20* cells might fail to express one or more genes critical for completion of nuclear division. To address this question, we sought suppressors of the temperature sensitivity of *hhf1-20*. We reasoned that if the mitotic arrest resulted from a general defect in gene expression, reflected in the Spt^- and Sin^- phenotypes, suppressors of the arrest should also revert the transcription phenotypes.

A high-copy yeast genomic library was screened for dosage suppressors of the temperature sensitivity of *hhf1-20*. In addition to the wild-type *HHF1* and *HHF2* histone H4 genes, we identified a gene that permitted growth of *hhf1-20* cells at the restrictive temperature. This gene turned out to be identical to

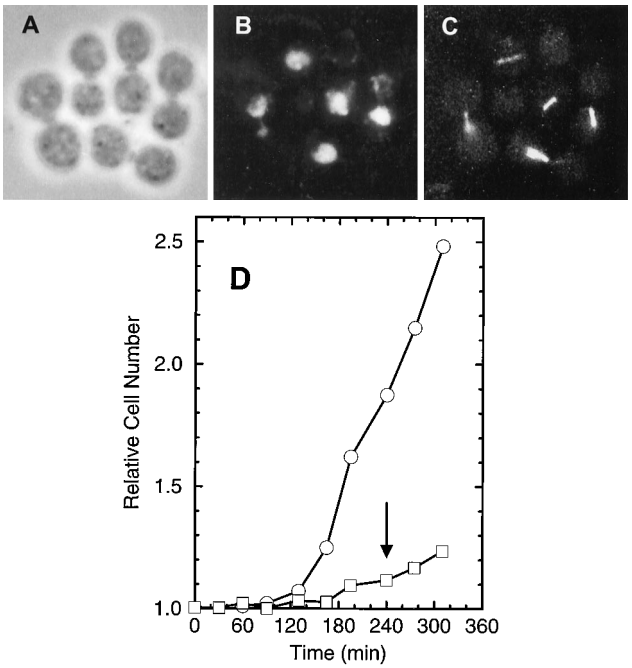

FIG. 9. Cell cycle morphology of *hhf1-20* cells from a synchronous culture at the restrictive temperature. (A) Phase-contrast image of arrested *hhf1-20* cells. (B) Fluorescence image of cells in panel A stained with DAPI for DNA. (C) Fluorescence image of cells in panel A stained for spindle morphology with an anti-tubulin antibody. Cells expressing the *hhf1-20* histone H4 allele arrest as large budded, dumbbell-shaped cells (A), with a single undivided nucleus (B) and a short bipolar spindle (C). (D) Cell division kinetics of synchronous cultures of *hhf1-20*. Early G_1 unbudded daughter cells were selected by centrifugal elutriation and used to establish two synchronously dividing cultures: one at 28°C (○) and the other at 37°C (□). The cells shown in panels A to C were harvested from the 37°C culture at 4 h (arrow).

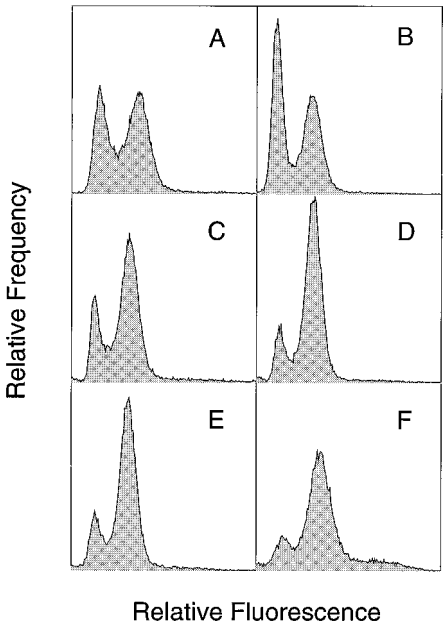

FIG. 10. DNA histograms of wild-type and *hhf1-20* cells. The DNA histograms determined by flow cytometry are shown for two strains that were isogenic except for their histone H4 genes. (A) Wild-type *HHF1* at 24°C in exponential growth. (B) Wild-type *HHF1* at 37°C in exponential growth. (C) Mutant *hhf1-20* at 24°C in exponential growth. (D) Mutant *hhf1-20* at 37°C for 90 min. (E) Mutant *hhf1-20* at 37°C for 3 h. (F) Mutant *hhf1-20* at 37°C for 8 h.

CSE4, which encodes a novel histone H3 variant similar to the mammalian kinetochore antigen CENP-A (81, 82). A complete description of the suppressor analysis and the genetic interaction of *CSE4* with histone H4 is in preparation (91). We next asked if this suppressor could cause reversion of the Spt^- transcription defect of *hhf1-20*. A high-copy plasmid carrying *CSE4* was introduced into the *hhf1-20 his4-912*δ *lys2-128*δ strain, and the transformant was examined for growth in the absence of histidine and lysine. As seen in Fig. 6, high-copy *CSE4* was unable to cause reversion of the Spt^- phenotype for either *his4-912*δ or *lys2-128*δ. These results suggest that the lethality of *hhf1-20* is unlikely to be an indirect result of a general defect in transcription.

DISCUSSION

In this report, we have described the isolation of a novel histone H4 mutant that is defective for nuclear division and mitotic chromosome transmission. Several observations indicate that *hhf1-20* is temperature sensitive for histone H4 function and not synthesis, assembly, or stability: (i) the temperature-sensitive phenotype was not suppressed by increased gene dosage; (ii) histone H4 remained stable in chromatin isolated from cells held at the restrictive temperature; (iii) cells remained viable at the restrictive temperature and could resume growth when returned to the permissive temperature; (iv) the oligonucleosome DNA ladder from nuclease digestion of *hhf1-20* chromatin was unaffected by temperature and did not show evidence of nucleosome depletion; and (v) the 2μm circle chromatin structure was temperature sensitive in cells arrested in G_1 prior to the synthesis or deposition of histone.

This is the first isolation of a temperature-sensitive lethal histone mutant by random mutagenesis and phenotypic screening in vivo. Together with the recent isolation of a cold-sensitive allele of the histone H2A gene *HTA1* (29), these conditional histone mutants provide important new reagents for genetic studies. The only conditional histone mutants previously available for study were those constructed by placing the gene under control of the inducible *GAL1* promoter (22, 40, 54). Such conditional null alleles have been of great utility in monitoring the consequences of nucleosome depletion (22, 40, 75), and for investigating the terminal phenotypes of synthetic lethal histone mutations (54). However, they are limited as genetic tools, particularly for identifying interacting components of chromatin and pseudoreversion analysis (33, 34).

The *hhf1-20* mutant is complex and depends on two amino acid substitutions: a lethal substitution in a DNA interaction domain and an intragenic suppressor substitution in helix 3 of the histone fold. These substitutions result in an unusual temperature-sensitive chromatin structure. At present, the molecular details of this change in chromatin structure are not known. At the restrictive temperature, the difference in mean topoisomer distribution of 2μm circle DNA between *HHF1* and *hhf1-20* is approximately 2.5 superhelical turns. Since each nucleosome confers about 1 negative superhelical turn to the DNA in chromatin, this difference could be accounted for by the loss of roughly two to three nucleosomes from the 2μm circle chromatin at the restrictive temperature. Depletion of 5 to 10% of the nucleosomes might be below the level of detection by micrococcal nuclease digestion of total chromatin. Alternatively, the difference in 2μm circle DNA might result from the integration of a small change in structure over all of the nucleosomes on the plasmid. The number of nucleosomes in 2μm circle chromatin has not been determined precisely but will be roughly 30 to 40 on the basis of the size of the 2μm circle DNA and the average repeat length of the yeast nucleosomal DNA. Thus, each nucleosome would have to increase the linking number of the 2μm circle DNA by about 0.06 to 0.08. This is well within the range of linking number change detected both within individual nucleosomes (25) and as the result of changes in histone acetylation (58). Theoretical considerations suggest that such changes can be accommodated by small alterations in core octamer structure (5). Further biophysical studies will be necessary to determine the molecular mechanism of the altered chromatin structure.

The immediate cause of the temperature sensitivity of *hhf1-20* is likely to be a mitotic defect. First, at the restrictive temperature, *hhf1-20* cells arrest at the G_2-M boundary just prior to nuclear division. Second, the mutant exhibits a temperature-dependent increase in the frequency of chromosome loss with no change in recombination. At semipermissive temperatures, this increase approaches 2 log units, and a further increase in this frequency at the fully restrictive temperature, summed over 16 chromosomes, would be sufficient to ensure eventual lethality. We considered two underlying mechanisms for the mitotic defect: a direct effect of altered chromatin structure and an indirect effect of aberrant gene transcription. Current evidence is more consistent with the chromatin structure model. First, none of the transcription phenotypes associated with *hhf1-20* were found to be temperature dependent; all were manifest at the permissive temperature, and they did

TABLE 3. Chromosome V loss and recombination in *hhf1-20*

Temp (°C)	Recombination frequency		Chromosome loss frequency	
	HHF1	*hhf1-20*	*HHF1*	*hhf1-20*
24	1.7×10^{-4}	4.4×10^{-4}	2.7×10^{-5}	1.2×10^{-4}
28	2.0×10^{-4}	1.5×10^{-4}	4.5×10^{-5}	8.3×10^{-5}
35	2.7×10^{-4}	2.7×10^{-4}	3.2×10^{-5}	1.5×10^{-3}

not increase or decrease in severity with increased temperature. Second, a dosage suppressor of the temperature sensitivity of *hhf1-20* did not suppress the Spt^- phenotype of the mutant. Finally, the strongest evidence comes from the nature of the dosage suppressor itself. *CSE4* was identified independently by Stoler et al. (81) as a recessive mutant that caused an increase in the frequency of mitotic chromosome nondisjunction. The gene encodes a novel histone H3 variant with similarities to the CENP-A mammalian kinetochore protein (82). Thus, the simplest interpretation of our results is that histone H4 and Cse4p interact via their histone fold domains to create a specialized chromatin structure at the centromeric DNA of eukaryotic chromosomes. In this model, at the restrictive temperature, *hhf1-20* produces a histone H4 that fails to interact properly with Cse4p and centromere DNA sequences, resulting in a loss of kinetochore function. High-copy expression of Cse4p overcomes this weakened interaction by driving formation of the Cse4p–Hhf1-20p protein complex and thus restoring sufficient kinetochore function to permit growth at the restrictive temperature. This model provides challenging predictions regarding centromere chromatin, and these are currently under investigation.

ACKNOWLEDGMENTS

We thank our colleagues for helpful discussions during the course of this work, D. Burke for anti-tubulin antibody, G. Fink and K. Arndt for yeast strains, and Chris Eichman and William Ross for expert technical assistance with the flow cytometry.

M.S.S. was supported by a fellowship from the Spanish Ministry of Education (Ministerio de Educación y Ciencia, Becas post-doctorales en el extranjero), and P.C.M. was supported in part by an ARCS Foundation fellowship, Metropolitan Washington chapter. This research was supported by National Institutes of Health grant GM28920 to M.M.S.

REFERENCES

1. **Aparicio, O. M., B. L. Billington, and D. E. Gottschling.** 1991. Modifiers of position effect are shared between telomeric and silent mating-type loci in *S. cerevisiae*. Cell **66:**1279–1287.
2. **Arents, G., R. W. Burlingame, B. C. Wang, W. E. Love, and E. N. Moudrianakis.** 1991. The nucleosomal core histone octamer at 3.1 A resolution: a tripartite protein assembly and a left-handed superhelix. Proc. Natl. Acad. Sci. USA **88:**10148–10152.
3. **Arents, G., and E. N. Moudrianakis.** 1993. Topography of the histone octamer surface: repeating 3-D motifs utilized in the docking of nucleosomal DNA. Proc. Natl. Acad. Sci. USA **90:**10489–10493.
4. **Arndt, K. T., C. A. Styles, and G. R. Fink.** 1989. A suppressor of a HIS4 transcriptional defect encodes a protein with homology to the catalytic subunit of protein phosphatases. Cell **56:**527–537.
5. **Bauer, W. R., J. J. Hayes, J. H. White, and A. P. Wolffe.** 1994. Nucleosome structural changes due to acetylation. J. Mol. Biol. **236:**685–690.
6. **Bavykin, S. G., S. I. Usachenko, A. O. Zalensky, and A. D. Mirzabekov.** 1990. Structure of nucleosomes and organization of internucleosomal DNA in chromatin. J. Mol. Biol. **212:**495–511.
7. **Bloom, K. S., E. Amaya, J. Carbon, L. Clarke, A. Hill, and E. Yeh.** 1984. Chromatin conformation of yeast centromeres. J. Cell Biol. **99:**1559–1568.
8. **Bloom, K. S., and J. Carbon.** 1982. Yeast centromere DNA is in a unique and highly ordered structure in chromosomes and small circular minichromosomes. Cell **29:**305–317.
9. **Boeke, J. D., F. LaCroute, and G. R. Fink.** 1984. A positive selection for mutants lacking orotidine-5′-phosphate decarboxylase activity in yeast: 5-fluoro-orotic acid resistance. Mol. Gen. Genet. **197:**345–346.
10. **Boeke, J. D., J. Trueheart, B. Natsoulis, and G. R. Fink.** 1987. 5-Fluoroorotic acid as a selective agent in yeast molecular genetics. Methods Enzymol. **154:**164.
11. **Brill, S. J., and R. Sternglanz.** 1988. Transcription-dependent DNA supercoiling in yeast DNA topoisomerase mutants. Cell **54:**403–411.
12. **Broach, J. R.** 1981. The yeast plasmid 2μ circle, p. 445–470. *In* J. N. Strathern, E. W. Jones, and J. R. Broach (ed.), The molecular biology of the yeast *Saccharomyces*: life cycle and inheritance. Cold Spring Harbor Laboratory Press, Cold Spring Harbor, N.Y.
13. **Brown, J. A., S. G. Holmes, and M. M. Smith.** 1991. The chromatin structure of *Saccharomyces cerevisiae* autonomously replicating sequences changes during the cell division cycle. Mol. Cell. Biol. **11:**5301–5311.
14. **Cairns, B. R., Y. Kim, M. H. Sayre, B. C. Laurent, and R. D. Kornberg.** 1994. A multisubunit complex containing the *SWI1*/*ADR6*, *SWI2*/*SNF2*, *SWI3*, *SNF5*, and *SNF6* gene products isolated from yeast. Proc. Natl. Acad. Sci. USA **91:**1950–1954.
15. **Carlson, M., and B. C. Laurent.** 1994. The SNF/SWI family of global transcriptional activators. Curr. Opin. Cell Biol. **6:**396–402.
16. **Clark-Adams, C. D., D. Norris, M. A. Osley, J. S. Fassler, and F. Winston.** 1988. Changes in histone gene dosage alter transcription in yeast. Genes Dev. **2:**150–159.
17. **Corliss, D. A., and W. E. White, Jr.** 1981. Fluorescence of yeast vitally stained with ethidium bromide and propidium iodide. J. Histochem. Cytochem. **29:** 45–48.
18. **Durrin, L. K., R. K. Mann, P. S. Kayne, and M. Grunstein.** 1991. Yeast histone H4 N-terminal sequence is required for promoter activation in vivo. Cell **65:**1023–1031.
19. **Fassler, J. S., and F. Winston.** 1988. Isolation and analysis of a novel class of suppressor of Ty insertion mutations in *Saccharomyces cerevisiae*. Genetics **118:**203–212.
20. **Funk, M., J. H. Hegemann, and P. Philippsen.** 1989. Chromatin digestion with restriction endonucleases reveals 150-160 bp of protected DNA in the centromere of chromosome 14 in *Saccharomyces cerevisiae*. Mol. Gen. Genet. **219:**153–160.
21. **Guacci, V., E. Hogan, and D. Koshland.** 1994. Chromosome condensation and sister-chromatid pairing in budding yeast. J. Cell Biol. **125:**517–530.
22. **Han, M., M. Chang, U. Kim, and M. Grunstein.** 1987. Histone H2B repression causes cell-cycle-specific arrest in yeast: effects on chromosomal segregation, replication, and transcription. Cell **48:**589–597.
23. **Hartwell, L. H., R. K. Mortimer. J. Culotti, and M. Culotti.** 1973. Genetic control of the cell division cycle in yeast. V. Genetic analysis of cdc mutants. Genetics **74:**267–286.
24. **Hartwell, L. H., and D. Smith.** 1985. Altered fidelity of mitotic chromosome transmission in cell cycle mutants of *S. cerevisiae*. Genetics **110:**381–395.
25. **Hayes, J. J., T. D. Tullius, and A. P. Wolffe.** 1990. The structure of DNA in a nucleosome. Proc. Natl. Acad. Sci. USA **87:**7405–7409.
26. **Hecht, A., T. Laroche, S. Strahlbolsinger, S. M. Gasser, and M. Grunstein.** 1995. Histone H3 and H4 N-termini interact with SIR3 and SIR4 proteins—a molecular-model for the formation of heterochromatin in yeast. Cell **80:**583–592.
27. **Herskowitz, I., B. Andrews, W. Kruger, J. Ogas, A. Sil, C. Coburn, and C. Peterson.** 1992. Integration of multiple regulatory inputs in the control of *HO* expression in yeast, p. 949–974. *In* S. L. McKnight and K. R. Yamamoto (ed.), Transcriptional regulation. Cold Spring Harbor Laboratory Press, Cold Spring Harbor, N.Y.
28. **Hieter, P., C. Mann, M. Snyder, and R. W. Davis.** 1985. Mitotic stability of yeast chromosomes: a colony color assay that measures nondisjunction and chromosome loss. Cell **40:**381–392.
29. **Hirschhorn, J. N., A. L. Bortvin, S. L. Ricupero-Hovasse, and F. Winston.** 1995. A new class of histone H2A mutations in *Saccharomyces cerevisiae* causes specific transcriptional defects in vivo. Mol. Cell. Biol. **15:**1999–2009.
30. **Hirschhorn, J. N., S. A. Brown, C. D. Clark, and F. Winston.** 1992. Evidence that SNF2/SWI2 and SNF5 activate transcription in yeast by altering chromatin structure. Genes Dev. **6:**2288–2298.
31. **Holm, C., T. Goto, J. C. Wang, and D. Botstein.** 1985. DNA topoisomerase II is required at the time of mitosis in yeast. Cell **41:**553–563.
32. **Holm, C., T. Stearns, and D. Botstein.** 1989. DNA topoisomerase II must act at mitosis to prevent nondisjunction and chromosome breakage. Mol. Cell. Biol. **9:**159–168.
33. **Huffaker, T. C., M. A. Hoyt, and D. Botstein.** 1987. Genetic analysis of the yeast cytoskeleton. Annu. Rev. Genet. **21:**259–284.
34. **Jarvik, J., and D. Botstein.** 1975. Conditional-lethal mutations that suppress genetic defects in morphogenesis by altering structural proteins. Proc. Natl. Acad. Sci. USA **72:**2738–2742.
35. **Jiang, Y. W., P. R. Dohrmann, and D. J. Stillman.** 1995. Genetic and physical interactions between yeast RGR1 and SIN4 in chromatin organization and transcriptional regulation. Genetics **140:**47–54.
36. **Jiang, Y. W., and D. J. Stillman.** 1992. Involvement of the *SIN4* global transcriptional regulator in the chromatin structure of *Saccharomyces cerevisiae*. Mol. Cell. Biol. **12:**4503–4514.
37. **Johnson, L. M., G. Fisher-Adams, and M. Grunstein.** 1992. Identification of a non-basic domain in the histone H4 N-terminus required for repression of the yeast silent mating loci. EMBO J. **11:**2201–2209.
38. **Johnson, L. M., P. S. Kayne, E. S. Kahn, and M. Grunstein.** 1990. Genetic evidence for an interaction between SIR3 and histone H4 in the repression of the silent mating loci in *Saccharomyces cerevisiae*. Proc. Natl. Acad. Sci. USA **87:**6286–6290.
39. **Kayne, P. S., U. J. Kim, M. Han, J. R. Mullen, F. Yoshizaki, and M. Grunstein.** 1988. Extremely conserved histone H4 N terminus is dispensable for growth but essential for repressing the silent mating loci in yeast. Cell **55:** 27–39.
40. **Kim, U. J., M. Han, P. Kayne, and M. Grunstein.** 1988. Effects of histone H4 depletion on the cell cycle and transcription of *Saccharomyces cerevisiae*. EMBO J. **7:**2211–2219.

41. **Kolodrubetz, D., M. C. Rykowski, and M. Grunstein.** 1982. Histone H2A subtypes associate interchangeably in vivo with histone H2B subtypes. Proc. Natl. Acad. Sci. USA **79:**7814–7818.
42. **Kornberg, R. D., and Y. Lorch.** 1992. Chromatin structure and transcription. Annu. Rev. Cell Biol. **8:**563–587.

42a. **Kruger, W., C. L. Peterson, A. Sil, C. Coburn, G. Arents, E. N. Moudrianakis, and I. Herskowitz.** 1995. Amino acid substitutions in the structured domains of histones H3 and H4 partially relieve the requirement of the yeast SWI/SNF complex for transcription. Genes Dev. **9:**2770–2779.

43. **Kunkel, T. A., J. D. Roberts, and R. A. Zakour.** 1987. Rapid and efficient site-specific mutagenesis without phenotypic selection. Methods Enzymol. **154:**367–382.
44. **Lambert, S. F., and J. O. Thomas.** 1986. Lysine-containing DNA-binding regions on the surface of the histone octamer in the nucleosome core particle. Eur. J. Biochem. **160:**191–201.
45. **Lee, M. S., and W. T. Garrard.** 1991. Positive DNA supercoiling generates a chromatin conformation characteristic of highly active genes. Proc. Natl. Acad. Sci. USA **88:**9675–9679.
46. **Lohr, D., and G. Ide.** 1979. Comparison of the structure and transcriptional capability of growing phase and stationary yeast chromatin: a model for reversible gene activation. Nucleic Acids Res. **6:**1909–1927.
47. **Longtine, M. S., S. Enomoto, S. L. Finstad, and J. Berman.** 1993. Telomere-mediated plasmid segregation in *Saccharomyces cerevisiae* involves gene products required for transcriptional repression at silencers and telomeres. Genetics **133:**171–182.
48. **Mann, R. K., and M. Grunstein.** 1992. Histone H3 N-terminal mutations allow hyperactivation of the yeast GAL1 gene in vivo. EMBO J. **11:**3297–3306.
49. **Marschall, L. G., and L. Clarke.** 1995. A novel cis-acting centromeric DNA element affects S. pombe centromeric chromatin structure at a distance. J. Cell Biol. **128:**445–454.
50. **Meeks-Wagner, D., and L. H. Hartwell.** 1986. Normal stoichiometry of histone dimer sets is necessary for high fidelity of mitotic chromosome transmission in *S. cerevisiae*. Cell **44:**43–52.
51. **Megee, P. C., B. A. Morgan, B. A. Mittman, and M. M. Smith.** 1990. Genetic analysis of histone H4: essential role of lysines subject to reversible acetylation. Science **247:**841–845.
52. **Megee, P. C., B. A. Morgan, and M. M. Smith.** 1995. Histone H4 and the maintenance of genome integrity. Genes Dev. **9:**1716–1727.
53. **Moretti, P., K. Freeman, L. Coodly, and D. Shore.** 1994. Evidence that a complex of SIR proteins interacts with the silencer and telomere binding-protein RAP1. Genes Dev. **8:**2257–2269.
54. **Morgan, B. A., B. A. Mittman, and M. M. Smith.** 1991. The highly conserved N-terminal domains of histones H3 and H4 are required for normal cell cycle progression. Mol. Cell. Biol. **11:**4111–4120.
55. **Morse, R. H.** 1991. Topoisomer heterogeneity of plasmid chromatin in living cells. J. Mol. Biol. **222:**133–137.
56. **Morse, R. H., D. S. Pederson, A. Dean, and R. T. Simpson.** 1987. Yeast nucleosomes allow thermal untwisting of DNA. Nucleic Acids Res. **15:**10311–10330.
57. **Norris, D., B. Dunn, and M. A. Osley.** 1988. The effect of histone gene deletions on chromatin structure in *Saccharomyces cerevisiae*. Science **242:**759–761.
58. **Norton, V. G., K. W. Marvin, P. Yau, and E. M. Bradbury.** 1990. Nucleosome linking number change controlled by acetylation of histones H3 and H4. J. Biol. Chem. **265:**19848–19852.
59. **Osborne, B. I., and L. Guarente.** 1988. Transcription by RNA polymerase II induces changes of DNA topology in yeast. Genes Dev. **9:**766–772.
60. **Park, E., and J. W. Szostak.** 1990. Point mutations in the yeast histone H4 gene prevent silencing of the silent mating-type locus *HML*. Mol. Cell. Biol. **10:**4932–4934.
61. **Pederson, D. S., and R. H. Morse.** 1990. Effect of transcription of yeast chromatin on DNA topology in vivo. EMBO J. **9:**1873–1881.
62. **Peterson, C. L., A. Dingwall, and M. P. Scott.** 1994. Five *SWI/SNF* gene products are components of a large multisubunit complex required for transcriptional enhancement. Proc. Natl. Acad. Sci. USA **91:**2905–2908.
63. **Peterson, C. L., and J. W. Tamkun.** 1995. The SWI-SNF complex: a chromatin remodeling machine? Trends Biochem. Sci. **20:**143–146.
64. **Polizzi, C., and L. Clarke.** 1991. The chromatin structure of centromeres from fission yeast: differentiation of the central core that correlates with function. J. Cell Biol. **112:**191–201.
65. **Prelich, G., and F. Winston.** 1993. Mutations that suppress the deletion of an upstream activating sequence in yeast: involvement of a protein kinase and histone H3 in repressing transcription in vivo. Genetics **135:**665–676.
66. **Pringle, J. R.** 1978. The use of conditional lethal cell cycle mutants for temporal and functional sequence mapping of cell cycle events. J. Cell. Physiol. **95:**393–405.
67. **Pringle, J. R.** 1981. The genetic approach to the study of the cell cycle, p. 3–28. *In* A. M. Zimmerman and A. Forer (ed.), Mitosis/cytokinesis. Academic Press, Inc., New York.
68. **Pringle, J. R., and L. H. Hartwell.** 1981. The *Saccharomyces cerevisiae* cell cycle, p. 97–142. *In* J. N. Strathern, E. W. Jones, and J. R. Broach (ed.), The molecular biology of the yeast *Saccharomyces*: life cycle and inheritance. Cold Spring Harbor Laboratory, Cold Spring Harbor, N.Y.
69. **Pulleyblank, D. E., M. Shure, D. Tang, J. Vinograd, and H. P. Vosberg.** 1975. Action of nicking-closing enzyme on supercoiled and nonsupercoiled closed circular DNA: formation of a Boltzmann distribution of topological isomers. Proc. Natl. Acad. Sci. USA **72:**4280–4284.
70. **Roth, S. Y., M. Shimizu, L. Johnson, M. Grunstein, and R. T. Simpson.** 1992. Stable nucleosome positioning and complete repression by the yeast $\alpha 2$ repressor are disrupted by amino-terminal mutations in histone H4. Genes Dev. **6:**411–425.
71. **Rykowski, M. C., J. W. Wallis, J. Choe, and M. Grunstein.** 1981. Histone H2B subtypes are dispensable during the yeast cell cycle. Cell **25:**477–487.
72. **Saavedra, R. A., and J. A. Huberman.** 1986. Both DNA topoisomerases I and II relax 2 micron plasmid DNA in living yeast cells. Cell **45:**65–70.
73. **Sandell, L. L., and V. A. Zakian.** 1993. Loss of a yeast telomere: arrest, recovery, and chromosome loss. Cell **75:**729–739.

73a. **Santisteban, M. S., and M. M. Smith.** Unpublished data.

74. **Saunders, M., M. Fitzgerald-Hayes, and K. Bloom.** 1988. Chromatin structure of altered yeast centromeres. Proc. Natl. Acad. Sci. USA **95:**175–179.
75. **Saunders, M. J., E. Yeh, M. Grunstein, and K. Bloom.** 1990. Nucleosome depletion alters the chromatin structure of *Saccharomyces cerevisiae* centromeres. Mol. Cell. Biol. **10:**5721–5727.
76. **Shortle, D., and D. Botstein.** 1983. Directed mutagenesis with sodium bisulfite. Methods Enzymol. **100:**457–468.
77. **Smith, M. M.** 1984. The organization of the yeast histone genes, p. 3–33. *In* G. S. Stein, J. L. Stein, and W. F. Marzluff (ed.), Histone genes. John Wiley & Sons, Inc., New York.
78. **Smith, M. M.** 1991. Mutations affecting nuclear proteins in yeast. Methods Cell Biol. **35:**485–523.
79. **Smith, M. M.** 1991. Histone structure and function. Curr. Opin. Cell Biol. **3:**429–437.
80. **Smith, M. M., and V. B. Stirling.** 1988. Histone H3 and H4 gene deletions in *Saccharomyces cerevisiae*. J. Cell Biol. **106:**557–566.
81. **Stoler, S., K. C. Keith, K. E. Curnick, and M. Fitzgerald-Hayes.** 1995. A mutation in CSE4, an essential gene encoding a novel chromatin-associated protein in yeast, causes chromosome nondisjunction and cell cycle arrest at mitosis. Genes Dev. **9:**573–586.
82. **Sullivan, K. F., M. Hechenberger, and K. Masri.** 1994. Human CENP-A contains a histone H3 related histone fold domain that is required for targeting to the centromere. J. Cell Biol. **127:**581–592.
83. **van Holde, K. E.** 1989. Chromatin. Springer-Verlag, New York.
84. **Weiher, H., and H. Schaller.** 1982. Segment-specific mutagenesis: extensive mutagenesis of a lac promoter/operator element. Proc. Natl. Acad. Sci. USA **79:**1408–1412.
85. **Weinert, T. A., and L. H. Hartwell.** 1988. The RAD9 gene controls the cell cycle response to DNA damage in *Saccharomyces cerevisiae*. Science **241:**317–322.
86. **Williamson, D., and D. Fennell.** 1975. The use of fluorescent DNA-binding agent for detecting and separating yeast mitochondrial DNA. Methods Cell Biol. **20:**335.
87. **Winston, F., and M. Carlson.** 1992. Yeast SNF/SWI transcriptional activators and the SPT/SIN chromatin connection. Trends Genet. **8:**387–391.
88. **Winston, F., D. T. Chaleff, B. Valent, and G. R. Fink.** 1984. Mutations affecting Ty-mediated expression of the *HIS4* gene of *Saccharomyces cerevisiae*. Genetics **107:**179–197.
89. **Wolffe, A. P.** 1992. Chromatin structure and function, p. 213. Academic Press, Inc., New York.
90. **Wright, J. H., D. E. Gottschling, and V. A. Zakian.** 1992. Saccharomyces telomeres assume a non-nucleosomal chromatin structure. Genes Dev. **6:**197–210.
91. **Yang, P., and M. M. Smith.** Unpublished data.